



Queensland University of Technology
Brisbane Australia

This may be the author's version of a work that was submitted/accepted for publication in the following source:

Pagnozzi, Alex, Dowson, Nicholas, Bourgeat, Pierrick, Rose, Stephen, [Bradley, Andrew](#), & Boyd, Roslyn
(2015)

Expectation-maximization with image-weighted Markov random fields to handle severe pathology.

In Suter, D (Ed.) *Proceedings of the 2015 International Conference on Digital Image Computing: Techniques and Applications (DICTA)*.

Institute of Electrical and Electronics Engineers Inc., United States of America, pp. 323-328.

This file was downloaded from: <https://eprints.qut.edu.au/114150/>

© Consult author(s) regarding copyright matters

This work is covered by copyright. Unless the document is being made available under a Creative Commons Licence, you must assume that re-use is limited to personal use and that permission from the copyright owner must be obtained for all other uses. If the document is available under a Creative Commons License (or other specified license) then refer to the Licence for details of permitted re-use. It is a condition of access that users recognise and abide by the legal requirements associated with these rights. If you believe that this work infringes copyright please provide details by email to qut.copyright@qut.edu.au

Notice: *Please note that this document may not be the Version of Record (i.e. published version) of the work. Author manuscript versions (as Submitted for peer review or as Accepted for publication after peer review) can be identified by an absence of publisher branding and/or typeset appearance. If there is any doubt, please refer to the published source.*

<https://doi.org/10.1109/DICTA.2015.7371257>

Expectation-maximization with image-weighted Markov Random Fields to handle severe pathology

Alex M. Pagnozzi, Nicholas Dowson,
Pierrick Bourgeat, Stephen Rose
The Australian e-Health Research Centre
CSIRO Digital Services & Productivity
Flagship
Brisbane, Australia
Email: Alex.Pagnozzi@csiro.au

Andrew P. Bradley
School of Information Technology and
Electrical Engineering
The University of Queensland
Brisbane, Australia

Roslyn N. Boyd
Queensland Cerebral Palsy and
Rehabilitation Research Centre
School of Medicine, The University of
Queensland
Brisbane, Australia

Abstract—This paper describes an automatic tissue segmentation algorithm for brain MRI of children with cerebral palsy (CP) who exhibit severe cortical malformations. Many of the currently popular brain segmentation techniques rely on registered atlas priors and so generalize poorly to severely injured data sets, because of large discrepancies between the target brain and healthy (or injured) atlases. We propose a prior-less approach combined with a modification of the Expectation Maximization (EM)/Markov Random Field (MRF) segmentation by imposing a continuous weighting scheme to penalize intensity discrepancies between pairs of neighbors within each clique neighborhood, to provide robustness to the unique clinical problem of severe anatomical distortion. This approach was applied to gray matter segmentations in 20 3D T1-weighted MRIs, of which 17 were of CP patients exhibiting severe malformation. We compare our adaptive algorithm to the popular ‘FreeSurfer’, ‘NiftySeg’, ‘FAST’ and ‘Atropos’ segmentations, which collectively are state-of-the-art surface deformation and EM approaches. The algorithm driven approach yielded improved segmentations (DSC 0.66 v 0.44 (FreeSurfer) v 0.60 (NiftySeg with 100% atlas prior relaxation) v 0.59 (FAST) v 0.64 (Atropos)) of the cerebral cortex relative to several ground-truth manual segmentations, when compared to the existing approaches.

Keywords—Magnetic resonance imaging; expectation maximization; Markov random field; cerebral palsy

I. INTRODUCTION

Cerebral palsy (CP) is a common physical disability (764,000 children in the USA) that can lead to both motor and cognitive impairment [1]. Magnetic resonance imaging (MRI) has a role in identifying the cerebral injury that underlies CP, and allowing quantitative image analysis techniques to develop models which link brain structure to patient function. One important class of injury observed in children with CP is cortical malformations, which present as a heterogeneous group of cortical shapes that lead to patient impairment [2]. An accurate segmentation of the gray matter is necessary to compute meaningful measures of the cortical surface that can be used to predict patient outcome and aid in implementing effective interventions. This remains a challenging task as the organization of the cortical surface can be significantly different in patients with severe developmental injury.

The Expectation Maximization (EM) algorithm [3] has frequently been used for the automated segmentation of brain MRI data [4], [5]. This approach allows for iteratively interleaved image bias correction [6], and a spatial consistency of labels through the Markov Random Field (MRF) [7]. It has been frequently applied to neonatal data sets [8]–[10] due to the robustness of the segmentation in the presence of high noise, significant partial volume effects, lack of tissue contrast, and extensive anatomical variability typical of these data sets. Despite EM being an adaptive approach, these studies typically utilize atlases to initialize the EM parameters, or iteratively scale the tissue probability of each voxel by the expected tissue prior from an atlas. To deal with anatomical variability, a non-rigid registration is performed to align the atlas priors to the data, and the influence of the atlas is subsequently reduced with a relaxation parameter that allows for more data-driven segmentation in later iterations [9], [10]. However in cases of severe injury, non-rigid registration typically fails and even with partial relaxation of the atlas priors, the discrepancies between the anatomical assumptions of the normative atlases and CP patients are too great to provide a robust initialization. Examples demonstrating the severity of injury that needs to be catered for are shown in Figure 1.

The limited relevance of atlas based priors for this application places more of the burden of accuracy on non-atlas priors defined by the clique potentials. Hence, in this paper, we propose a modification to the formulation of the local clique potentials within the adaptive EM algorithm to enable an improved segmentation of the cerebral cortex in the structural MRI of children with CP. Using 20 T1-weighted MRIs of children, of which 17 were CP patients exhibiting severe cortical malformations, the proposed approach was compared to four widely used methods: FreeSurfer [11], NiftySeg [10], FSL’s FAST [7]) and ANT’s Atropos [12]. The FreeSurfer software uses a data-driven deformable surface approach, initialized by registration to an atlas, to detect the inner and outer surfaces of the cortical gray matter, while NiftySeg, FAST and Atropos use an EM segmentation algorithm with an incorporated MRF and interleaved bias correction. We demonstrate that our proposed approach is able to accurately model the cerebral cortex in the presence of large

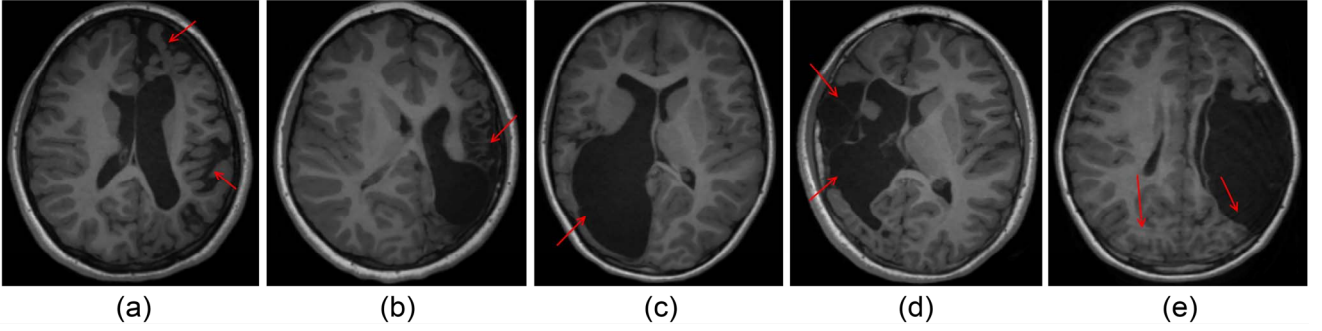


Figure 1. An illustration of extensive injury common in CP patients: (a-b) cortical malformation and (c-e) ventriculomegaly. Regions of injury or artifact are highlighted by red arrows.

injury variability, in comparison to FreeSurfer, NiftySeg, FAST and Atropos.

II. MATERIALS AND METHODS

A. Subjects

The data were acquired from two different scanners, and with three different sets of scanning parameters, including a 3T Siemens' scanner (TR = 1900 ms, TE = 2.32 ms, flip angle = 9 degrees), a 1.5T GE scanner with two different scanning parameters; (TR = 12.36 ms, TE = 5.17 ms, flip angle = 13 degrees) and (TR = 124.29 ms, TE = 4.37 ms, flip angle = 10 degrees). All data was acquired with the appropriate institutional ethics approval. A total of 20 T1-weighted volumes were analyzed, of which 17 were patients with CP. The mean age at the time of the scan was 12.26 ± 2.48 years (range 7-17 years), while the male to female ratio was 9/11. The images were manually segmented on the hemisphere of injury by two raters.

B. Preprocessing

Bias correction was performed by the N4 algorithm [13]. All images were then aligned using an affine block matching registration algorithm [14] to the Colin 27 Average Brain Atlas. Image denoising was performed using anisotropic diffusion [15] with modified curvature diffusion equation [16]. This was critical to reduce the influence of image noise in the subsequent weighted clique potential. Skull stripping was performed in MATLAB (Mathworks, Natick, MA) using an approach that identified intracranial cerebrospinal fluid (CSF) at locations proximal to the skull using intensity thresholding. Brain tissue was segmented as the region encapsulated by this intracranial CSF segmentation, with morphological operations implemented to ensure consistent segmentations between adjacent MR slices.

C. Expectation Maximization Algorithm

The adaptive EM algorithm [3] has been successfully used in a number of studies [4], [5], [7] for segmenting T1-weighted images. In these approaches, the segmentation problem is formulated as an incomplete data problem where given the set of n voxel intensities in the image, $y = \{y_i, i \in [1; n]\}$, the algorithm attempts to compute a set of labels, $z = \{z_i, i \in [1; K]\}$, describing which of K tissue classes each voxel belongs, with k denoting a specific tissue class $1 \leq k \leq K$.

Voxels are indexed by i . Intensity distributions for each tissue class k are parameterized by the Gaussian mean and standard deviation $\Phi_k = (\mu_k, \sigma_k)$. The estimation of the maximum likelihood parameters, Φ , is obtained by interleaving the estimation of the hidden segmentation, z , (E-step), followed by the update of the class distributions, Φ , based on the observed image y and segmentation z (M-step).

Prior to the EM, Φ is initialized using a peak finding algorithm that searches the intensity histogram for the two sufficiently separated dominant peaks from the brain mask, which are labeled as gray and white matter. The mean intensity of the CSF distribution is estimated by searching backwards from the gray matter peak. The standard deviation of each distribution is computed from the gradient of the Gaussian intensity distribution on either side of the respective maximum.

In the E-step, tissue labels at each voxel, i , are selected as the tissue class k that has the minimum posterior likelihood p_{ik} , which at iteration $m + 1$ takes the form:

$$p_{ik}^{(m+1)} = \frac{\frac{1}{\sqrt{2\pi\sigma_k^2}} \exp\left(-\frac{y_i - \mu_k}{2\sigma_k^2}\right) f(z|\Phi_z)}{\sum_{j=1}^K \left[\frac{1}{\sqrt{2\pi\sigma_j^2}} \exp\left(-\frac{y_i - \mu_j}{2\sigma_j^2}\right) f(z|\Phi_z) \right]} \quad (1)$$

Given a set of labels z , the parameters are updated in the M-step as follows:

$$\mu_k^{(m+1)} = \frac{\sum_i^n p_{ik}^{(m+1)} y_i}{\sum_i^n p_{ik}^{(m+1)}} \quad (2)$$

$$(\sigma_k^{(m+1)})^2 = \frac{\sum_i^n p_{ik}^{(m+1)} (y_i - \mu_k^{(m+1)})^2}{\sum_i^n p_{ik}^{(m+1)}} \quad (3)$$

The form of $f(z|\Phi_z)$ in (1), which is related to the MRF implementation, is critical to the performance of the algorithm. The modification of this term is the contribution of this paper, which is proposed in order to provide robustness to the segmentation of MRI scans with extensive CP-related injuries, as described in the next subsection.

D. Gradient weighted MRF

The calculation of (1) in the EM approach includes consideration of the spatial relationship between a voxel and

its six adjacent neighbors. It is assumed that the incorporated random field follows a Gibbs distribution:

$$f(z|\Phi_z) = Z(\Phi_z)^{-1} \exp(-U_{mrf}), \quad (4)$$

where $Z(\Phi_z) = \sum_z \exp(-U_{mrf})$ is called the partition function and U_{mrf} is called the energy function. The energy function is formulated as the sum of clique potentials $V_c(z)$ over all possible cliques, C :

$$U_{mrf}(z) = \sum_{c \in C} V_c(z). \quad (5)$$

Traditionally, clique potentials simply compute the sum of mismatched labels between the voxel x_i and the neighbors in the clique:

$$V_c(z_i, z_j) = \begin{cases} \frac{1}{2} & \text{if } z_i \neq z_j \\ 0 & \text{if } z_i = z_j \end{cases} \quad (6)$$

This standard formulation of the clique potential is implemented in the Atropos software [12]. More sophisticated modulation of MRF parameters are proposed in the seminal works of Geman and Geman, and Mumford and Shah [17], [18]. These techniques modulate clique potentials based on gradients or smooth edges in the label field, z , respectively. Both FSL's FAST and NiftySeg use a clique potential discretely weighted by gradients in the label field, as in Geman and Geman [17].

To compensate for the lack of an informative atlas-based prior, the proposed approach instead incorporates a new assumption in the model, that a mismatch of labels at a clique edge will have an associated mismatch of intensity at defined tissue boundaries. Contrary to previous studies, in the proposed modification the cost of neighboring voxels with different labels is scaled down by the presence of intensity gradients between the voxels in the image, y . Correspondingly, the cost of neighboring voxels with identical labels is scaled up in the presence of intensity gradients between the voxels. Hence, in the modified MRF the cost of neighboring labels is weighted by the gradient of intensity between the neighboring voxels, which is congruous with the concept that different labels in a clique should have a different intensity, and vice versa. Therefore the cost of neighboring voxels as follows:

$$V_c(z_i, z_j) = \begin{cases} \frac{1}{2} \left(\exp\left(-\frac{|y_i - y_j|}{s}\right) \right) & \text{if } z_i \neq z_j \\ \frac{1}{2} \left(1 - \exp\left(-\frac{|y_i - y_j|}{s}\right) \right) & \text{if } z_i = z_j \end{cases} \quad (7)$$

In (7), s is a free parameter that can be adjusted based on the gradient across tissue boundaries present in the MRI. This parameter was chosen to be half of the difference in intensity between WM and GM at initialization, which was consistent due to intensity normalization in MRI pre-processing.

We note that using intensity gradients to weight clique potentials is common in graph cut image segmentation [19], which has previously been applied to brain segmentation [20], [21]. The benefit of the proposed weighted MRF formulation, however, is that incorporating intensity information within the

MRF assists in the optimisation of the interleaved EM-based segmentation in cases where voxel-wise atlas priors cannot be provided.

III. RESULTS

To assess the accuracy of the gray matter segmentations, the segmentations obtained from the proposed EM approach with the gradient weight MRF were compared to the manual segmentations performed by two raters using the Dice Similarity Coefficient (DSC) metric [22]. In addition, the segmentations obtained from the EM approach with the standard MRF formulation of (6), FreeSurfer, NiftySeg, FAST and Atropos were compared. The NiftySeg algorithm was run twice, once using the default relaxation of the atlas priors, and once with the relaxation parameter set to its maximum. In this second implementation, atlas priors are still used to initialize tissue distributions, but the atlas priors were subsequently given zero weight during EM optimization. The mean DSC of the two raters for each method are reported in Table 1. Not all the data was segmented by rater 2 and is indicated by a dash in the inter-rater reliability column. The gray matter segmentations provided by these approaches for a typical subject is illustrated in Figure 2.

The data was divided into the 3 healthy cases and the 17 cases with injury. The proposed approach gave comparable performance (0.773) to the best performing approach among the healthy data, and gave the best performance among the injured data (0.655). NiftySeg with 100% relaxation obtained the best performance among the healthy data (0.775), but a substantially reduced DSC for the 17 injured cases (0.596). In all injured cases, NiftySeg with 100% relaxation was in greater agreement with the manual raters compared to the default relaxation of priors, highlighting the deleterious effect of using atlases on scans containing injury. Atropos gave the second highest performance among the injured data (0.632). Neither FreeSurfer nor the classic MRF implementation demonstrated performance comparable to the proposed approach. Overall, the proposed approach consistently had the best performance: in 10 of the 20 cases, versus 6 cases for 100% relaxed NiftySeg, two cases for classic MRF and two cases for Atropos.

In all cases, the inter-rater reliability was greater than the DSC obtained for any of the methods. The agreement between the raters went as low as 0.662, which was largely due to local reductions in the contrast between the gray and white matter, obscuring the tissue boundary. An illustration of the segmentations obtained from the several methods from an image containing severe injury is shown in Figure 2.

IV. DISCUSSION

The proposed approach outperformed all the other state-of-the-art EM methods with integrated atlas priors on the cases with cortical injury, demonstrating the potentially deleterious effect of incorporating atlas-based priors when segmenting scans with severe injury. This improvement is the result of the weighted MRF, which provides additional robustness by forcing the labeling to be consistent with intensity gradients in the image. The benefit of the modified MRF is demonstrated

by the slightly reduced DSC's obtained using the EM with the standard MRF, as this approach computes high neighbor costs at tissue boundaries. Consequently, thin extensions of white

matter or CSF are smoothed over and labeled as gray matter using this method, as is shown in Figure 2(d).

TABLE I. MEAN DSC RESULTS COMPARING THE SEGMENTATIONS OBTAINED FROM THE PROPOSED EM AND WEIGHTED MRF APPROACH, EM WITH THE STANDARD MRF, FREE SURFER, NIFTYSEG WITH DEFAULT AND 100% RELAXATION OF ATLAS PRIORS, FAST AND ATROPOS WITH THE MANUAL SEGMENTATIONS OBTAINED FROM TWO RATERS. INTER-RATER RELIABILITY IS PROVIDED BASED ON THE DSC OVERLAP BETWEEN THE SEGMENTATIONS FROM THE TWO RATERS. FOR EACH PATIENT, THE LARGEST DSC IS IN BOLD.

Subject Age	EM - weighted MRF	EM - standard MRF	Free-Surfer	NiftySeg	NiftySeg 100% relaxation	FSL's FAST	ANT's Atropos	Inter-rater reliability
<i>Healthy cases</i>								
8	0.776	0.628	0.473	0.767	0.791	0.761	0.737	0.813
12	0.810	0.694	0.489	0.791	0.804	0.735	0.741	0.825
15	0.732	0.642	0.536	0.700	0.729	0.684	0.692	-
Mean DSC	0.773	0.654	0.499	0.753	0.775	0.727	0.723	0.819
<i>Cases with cortical injury</i>								
7	0.739	0.432	NA	0.567	0.569	0.601	0.695	0.749
9	0.707	0.681	NA	0.677	0.696	0.698	0.712	0.745
10	0.351	0.357	NA	0.312	0.324	0.146	0.355	-
10	0.716	0.636	0.568	0.711	0.727	0.702	0.687	0.813
10	0.559	0.585	NA	0.423	0.441	0.522	0.542	0.730
12	0.625	0.601	0.458	0.457	0.472	0.553	0.644	0.634
12	0.681	0.429	0.365	0.417	0.419	0.548	0.668	-
13	0.651	0.627	0.472	0.468	0.489	0.610	0.622	-
13	0.725	0.600	NA	0.708	0.720	0.674	0.717	0.771
13	0.610	0.564	NA	0.518	0.547	0.508	0.563	0.662
14	0.714	0.543	0.242	0.724	0.748	0.683	0.683	0.802
14	0.664	0.428	0.486	0.628	0.650	0.646	0.647	0.714
14	0.700	0.671	0.348	0.671	0.705	0.632	0.665	0.737
14	0.741	0.735	0.537	0.656	0.682	0.673	0.701	-
14	0.640	0.637	NA	0.575	0.585	0.596	0.613	-
15	0.654	0.443	0.461	0.645	0.656	0.581	0.647	0.672
15	0.657	0.523	0.480	0.671	0.697	0.674	0.654	0.695
Mean DSC	0.655	0.558	0.442	0.578	0.596	0.591	0.632	0.727

The limitation of using atlas priors for segmentation in the presence of injury is illustrated in Figure 2(f-g). Specifically in Fig. 2(g), due to the extreme anatomical malformations, much of the CSF was incorrectly labeled as gray matter during initialization, resulting in poor and irrecoverable initial estimates of distribution. The same issue resulted in one injured case where the DSC<0.2 was observed for FAST. Although this highlights the limitation of atlases to initialize prior tissue distributions, many atlas-based segmentation algorithms accommodate pathologies using a local relaxation of atlas priors [23], [24]. These approaches, while validated on data with brain tumors, have unique challenges in the CP setting, where the region of severe malformation may include

gray matter that needs to be continuously segmented along with healthy regions of gray matter, and not as a separate tumor entity. In the proposed EM-weighted MRF implementation, a straightforward peak-finding algorithm was instead used to robustly estimate initial tissue distributions, assisting an accurate segmentation of cortical gray matter in injured cases. Alternative approaches, such as Otsu thresholding [25] or fuzzy c-means [26], could similarly provide robust tissue distribution initializations. These methods are used for initialization in the Atropos software [12], potentially accounting for its second-highest performance among the injured cases.

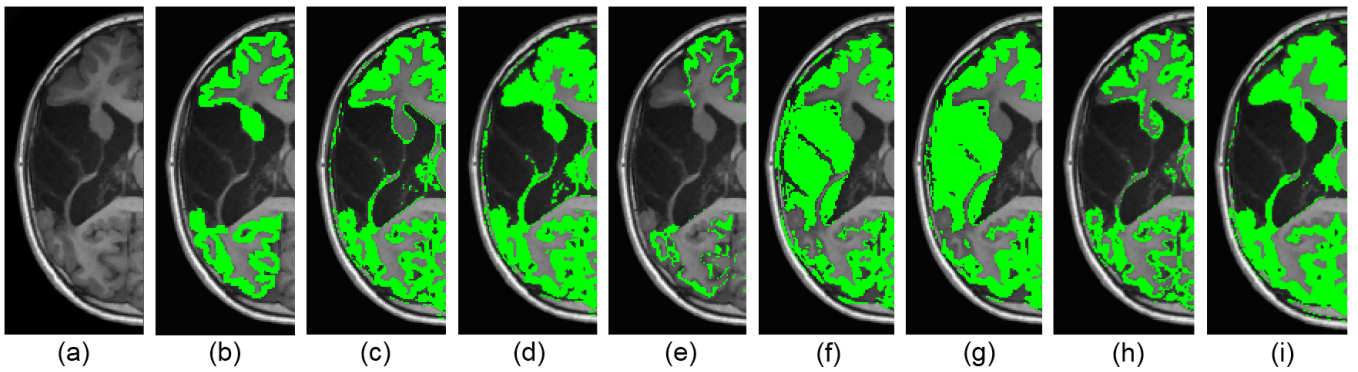


Figure 2. (a) An axial slice of a patient with cortical injury, and the cortical gray matter segmentations obtained from the (b) manual rater, (c) EM-weighted MRF, (d) EM-standard MRF, (e) FreeSurfer software, (f) NiftySeg, (g) NiftySeg with 100% prior relaxation, (h) FAST and (i) Atropos.

FreeSurfer failed to produce a result (NA in Table 1) on seven of the 20 MRI scans, corresponding to data sets exhibiting more severe injury causing failure in the deformation of the cortical surface. For the remaining scans, the presence of injury was observed to impact the deformation of the cortical surfaces. This is illustrated in Figure 2(e), where the presence of injury affected the deformable surface such that it does not accurately represent the gray matter from Figure 2(a).

Even in healthy brains, the segmentation of cortical gray matter is challenging with DSC's of ~ 0.8 reported in the few available references [8], [9], [27], due to the narrow and complex morphology of cortical GM and partial volume effects. The extensive injuries typical of CP compound this, making the distinction between gray and white matter ambiguous and impacting on the DSC. Additionally, for the cases where DSC's of 0.351 and 0.559 were obtained using the proposed approach, the overlap measure was impacted due to the significant absence of gray matter on the injured side.

A limitation of this work is that the proposed modification has only been applied to the segmentation of tissue types, with specific focus on improving cortical grey matter segmentations. As shown in Figure 2(c), the proposed modification mislabels the caudate nucleus. Anatomical parcellation requires the use of *a priori* information provided by atlas-based methods.

In summary, the results highlight the challenges of using atlas-based priors in cases of severe injury, as healthy atlases do not generalize to unhealthy cases and even sophisticated non-rigid registration algorithms like that used by NiftySeg, FAST or Atropos cannot compensate for severe changes in anatomy. This places the burden of obtaining robust segmentations on the design of the clique weighting function as opposed to dictating a need for more training data. Although relatively simple adaptive approaches such as the proposed modified MRF can yield a robustness to severe pathology or injury, atlas-based approaches are still necessary to perform subcortical anatomical, or gyral, labeling, that EM segmentation approaches alone cannot accurately replicate. The authors also note that sufficient data coupled with an efficient atlas selection and relaxation strategy could also yield improvements to the results obtained. Therefore, future

investigations applying atlas-based approaches to images containing severe pathology should consider using simple, adaptive algorithms for initializing tissue distribution estimates, or modifying the posterior likelihood estimation via the neighborhood potential, for providing additional robustness.

V. CONCLUSION

In this paper we have described a modification to the EM-MRF approach tailored specifically for the automated cortical gray matter segmentation of MRI of children with CP. The extensive anatomical malformations caused by injury related to CP limit the utility of atlas based priors. To impart robustness to the formulation of the posterior likelihood, and to compensate for the limited relevance of atlas priors, the clique potentials in the MRF were modified to include penalization for mismatched labels over low intensity gradients, and matched labels over high intensity gradients. The result is an improved segmentation at the boundary of cerebral tissues in a cohort of patients with severe CP-related injury in comparison to four state-of-the-art segmentation methods: FreeSurfer, NiftySeg, FAST and Atropos. In future, we recommend atlas-based approaches take advantage of robust initialization methods and modified neighborhood potentials to provide greater robustness to injury.

ACKNOWLEDGMENT

Alex Pagnozzi is supported by the Australian Postgraduate Award (APA) from The University of Queensland, and a stipend from the Commonwealth Scientific Industrial and Research Organisation (CSIRO). Roslyn Boyd is supported by a NHMRC Career Development Fellowship (1037220) and a NHMRC Project Grant COMBIT (1003887). Andrew Bradley is supported by an ARC Future fellowship (FT110100623). No other authors have potential conflicts of interest to declare.

REFERENCES

- [1] E. Blair and L. Watson, "Epidemiology of cerebral palsy.," *Semin. Fetal Neonatal Med.*, vol. 11, no. 2, pp. 117–25, Apr. 2006.
- [2] R. Guerrini and W. B. Dobyns, "Malformations of cortical development: clinical features and genetic causes.," *Lancet. Neurol.*, vol. 13, no. 7, pp. 710–26, Jul. 2014.

- [3] A. P. Dempster, N. M. Laird, and D. B. Rubin, "Maximum likelihood from incomplete data via the EM algorithm," *J. R. Stat. Soc. Ser. B*, vol. 39, no. 1, pp. 1–38, 1977.
- [4] W. M. Wells, W. L. Grimson, R. Kikinis, and F. a Jolesz, "Adaptive segmentation of MRI data.," *IEEE Trans. Med. Imaging*, vol. 15, no. 4, pp. 429–42, Jan. 1996.
- [5] K. Van Leemput, F. Maes, D. Vandermeulen, and P. Suetens, "Automated model-based tissue classification of MR images of the brain.," *IEEE Trans. Med. Imaging*, vol. 18, no. 10, pp. 897–908, Oct. 1999.
- [6] K. M. Pohl, W. M. Wells, A. Guimond, K. Kasai, M. E. Shenton, R. Kikinis, W. E. L. Grimson, and S. K. Warfield, "Incorporating Non-rigid Registration into Expectation Maximization Algorithm to Segment MR Images," in *Medical Image Computing and Computer-Assisted Intervention — MICCAI 2002*, 2002, p. pp 564–571.
- [7] Y. Zhang, M. Brady, and S. Smith, "Segmentation of brain MR images through a hidden Markov random field model and the expectation-maximization algorithm," *IEEE Trans. Med. Imaging*, vol. 20, no. 1, pp. 45–57, Jan. 2001.
- [8] M. Murgasova, L. Dyet, D. Edwards, M. Rutherford, J. V. Hajnal, and D. Rueckert, "Segmentation of Brain MRI in Young Children," in *Medical Image Computing and Computer-Assisted Intervention—MICCAI 2006*, 2006, p. pp 687–694.
- [9] A. Makropoulos, C. Ledig, P. Aljabar, A. Serag, J. V. Hajnal, A. D. Edwards, A. Serena J. Counsell, and D. Rueckert, "Automatic tissue and structural segmentation of neonatal brain MRI using Expectation-Maximization," in *MICCAI Grand Challenge: Neonatal Brain Segmentation 2012 (NeoBrainS12)*, 2012.
- [10] M. J. Cardoso, A. Melbourne, G. S. Kendall, M. Modat, C. F. Haggmann, N. J. Robertson, N. Marlow, and S. Ourselin, "Adaptive Neonate Brain Segmentation," in *Medical Image Computing and Computer-Assisted Intervention—MICCAI 2011*, 2011, p. pp 378–386.
- [11] B. Fischl, "FreeSurfer.," *Neuroimage*, vol. 62, no. 2, pp. 774–81, Aug. 2012.
- [12] B. B. Avants, N. J. Tustison, J. Wu, P. A. Cook, and J. C. Gee, "An open source multivariate framework for n-tissue segmentation with evaluation on public data.," *Neuroinformatics*, vol. 9, no. 4, pp. 381–400, Dec. 2011.
- [13] N. J. Tustison, B. B. Avants, P. A. Cook, Y. Zheng, A. Egan, P. A. Yushkevich, and J. C. Gee, "N4ITK: improved N3 bias correction.," *IEEE Trans. Med. Imaging*, vol. 29, no. 6, pp. 1310–20, Jun. 2010.
- [14] D. Rivest-Hénault, N. Dowson, P. Greer, and J. Dowling, "Inverse-consistent rigid registration of CT and MR for MR-based planning and adaptive prostate radiation therapy," *J. Phys. Conf. Ser.*, vol. 489, no. 1, p. 012039, Mar. 2014.
- [15] P. Perona and J. Malik, "Scale-space and edge detection using anisotropic diffusion," *IEEE Trans. Pattern Anal. Mach. Intell.*, vol. 12, no. 7, pp. 629–639, Jul. 1990.
- [16] A. Yezzi, "Modified curvature motion for image smoothing and enhancement," *IEEE Trans. Image Process.*, vol. 7, no. 3, pp. 345–352, 1998.
- [17] S. Geman and D. Geman, "Stochastic Relaxation, Gibbs Distributions, and the Bayesian Restoration of Images," *IEEE Trans. Pattern Anal. Mach. Intell.*, vol. PAMI-6, no. 6, pp. 721–741, Nov. 1984.
- [18] D. Mumford and J. Shah, "Optimal approximations by piecewise smooth functions and associated variational problems," *Commun. Pure Appl. Math.*, vol. 42, no. 5, pp. 577–685, Jul. 1989.
- [19] Y. Boykov, O. Veksler, and R. Zabih, "Fast approximate energy minimization via graph cuts," *IEEE Trans. Pattern Anal. Mach. Intell.*, vol. 23, no. 11, pp. 1222–1239, 2001.
- [20] J. M. Lötjönen, R. Wolz, J. R. Koikkalainen, L. Thurfjell, G. Waldemar, H. Soininen, and D. Rueckert, "Fast and robust multi-atlas segmentation of brain magnetic resonance images.," *Neuroimage*, vol. 49, no. 3, pp. 2352–65, Feb. 2010.
- [21] Z. Song, N. Tustison, B. Avants, and J. C. Gee, "Integrated Graph Cuts for Brain MRI Segmentation," in *Medical Image Computing and Computer-Assisted Intervention - MICCAI 2006*, 2006, pp. 831–838.
- [22] L. R. Dice, "Measures of the Amount of Ecologic Association Between Species," *Ecology*, Vol. 26, No. 3, 1945. [Online]. Available: <http://www.jstor.org/stable/1932409>. [Accessed: 01-Sep-2014].
- [23] S. Parisot, H. Duffau, S. Chemouny, and N. Paragios, "Joint Tumor Segmentation and Dense Deformable Registration of Brain MR Images," in *Medical Image Computing ...*, N. Ayache, H. Delingette, P. Golland, and K. Mori, Eds. Springer Berlin Heidelberg, 2012, pp. 651–658.
- [24] S. Parisot, W. Wells, S. Chemouny, H. Duffau, and N. Paragios, "Concurrent tumor segmentation and registration with uncertainty-based sparse non-uniform graphs.," *Med. Image Anal.*, vol. 18, no. 4, pp. 647–59, May 2014.
- [25] N. Otsu, "A threshold selection method from gray-level histograms.," *Automatica*, vol. 11, pp. 23–27, 1975.
- [26] J. C. Bezdek, R. Ehrlich, and W. Full, "FCM \square : The fuzzy c-means clustering algorithm," *Comput. Geosci.*, vol. 10, no. 2, pp. 191–203, 1984.
- [27] A. Melbourne, M. J. Cardoso, G. S. Kendall, N. J. Robertson, N. Marlow, and S. Ourselin, "NeoBrainS12 Challenge: Adaptive neonatal MRI brain segmentation with myelinated whitematter class and automated extraction of ventricles I-IV," in *MICCAI Grand Challenge: Neonatal Brain Segmentation 2012 (NeoBrainS12)*, 2012, p. 16.